Electrical characterization of thin InAs films grown on patterned W/GaAs substrates

Astromskas, Gvidas; Wallenberg, Reine; Wernersson, Lars-Erik

Published in:
Journal of Vacuum Science and Technology B

DOI:
10.1116/1.3222859

2009

Electrical characterization of thin InAs films grown on patterned W/GaAs substrates

Gvidas Astromskas[a)]
Solid State Physics, Lund University, Box 118, S-22100 Lund, Sweden

L. Reine Wallenberg
Polymer and Materials Chemistry/nCHREM, Lund University, Box 118, S-22100 Lund, Sweden

Lars-Erik Wernersson
Solid State Physics, Lund University, Box 118, S-22100 Lund, Sweden

(Received 25 April 2008; accepted 10 August 2009; published 15 September 2009)

InAs has been grown on W–GaAs patterned substrates using metal organic vapor phase epitaxy. It is shown that the W pattern guides the nucleation of the InAs on the GaAs substrate and that the islands formed may be used to embed metal features in a hybrid InAs/GaAs structure. A lower resistance (factor of 2) was measured for the hybrid structures as compared to reference structures. The reduction in the resistance is attributed to an increased carrier concentration as observed from Hall measurements on devices with different tungsten densities. Cross-sectional transmission electron microscopy investigations reveal a void-free overgrowth above the metal despite the large mismatch of the InAs/GaAs system. © *2009 American Vacuum Society.* [DOI: 10.1116/1.3222859]

I. INTRODUCTION

Materials with a narrow band gap are attractive for high-speed devices and long wavelength optical devices. For instance, high electron mobility transistors[1] and lasers operating above 2 μm (Ref. 2) have been fabricated in materials lattice matched to InAs or GaSb. Due to the lack of semi-insulating substrates, the layers are typically grown on GaAs or InP semi-insulating substrates using thick and complex buffer layers. In a typical process, the initial stage of the deposition results in a highly defective layer close to the interface, where the strain is released via dislocation formation. As the deposition continues, the number of defects is reduced and the material quality improves. Eventually, epitaxial layers suitable for device fabrication may be obtained.

In this article, we present an alternative technology in that we grow InAs on a patterned W–GaAs substrate. We show that the W pattern affects the growth of the InAs both in the nucleation stage and by subsequent lateral overgrowth over the metal and that the electrical properties of the layer are influenced by the presence of the W layer. These results are discussed in terms of surface carrier accumulation around the W pattern.

II. MATERIALS AND METHODS

The fabrication of the W–GaAs patterns for the overgrowth is based on a lift-off process using evaporated metal.[3] The patterns formed consist of lines (width of 90–100 nm and periods of 200–700 nm) and concentric rings (width of 100 nm and periods of 400 nm). Metal organic vapor phase epitaxy (MOVPE) was used to epitaxially overgrow the patterned substrates with InAs at a growth temperature of 500 °C and a V/III ratio of 14. Trimethylindium (TMI) and arsine (AsH_3) were used as sources for the InAs growth at a MOVPE reactor pressure of 100 mbars. The molar fractions of the TMI and AsH_3 were 2.75×10^{-5} and 3.74×10^{-4}, respectively, and the total flow was 6000 slm (standard liters per minute). After the growth, the samples were inspected using scanning electron microscopy (SEM) to evaluate the quality of the deposited material. Atomic force microscopy (AFM) measurements were performed to extract the thickness of the overgrown layer. At these growth conditions, no deposition occurred on the tungsten structures and thus larger W patterns were used as references when measuring the thickness of the InAs layer. After thickness determination, device mesas were processed. For the electrical characterization of the InAs/W/GaAs integrated structure, patterns with 70-μm-long tungsten wires oriented 30° off the $[0\bar{1}1]$ direction were used. These gratings had different periods, 200–700 nm, and different metal widths, 70–90 nm. Electron beam lithography (EBL) was used to align and expose mesa patterns on the sample, employing positive EBL resist polymethyl methacrylate. Mesa structures were formed by etching the developed sample down to the semi-insulating GaAs using $H_3PO_4:H_2O_2:H_2O$. The depth of the etching was controlled using profilometer scans, as the etching solution attacks both InAs and GaAs. EBL was finally used to align contacting pads with the etched mesas. Au:Ti layers (500:5 nm thick) were evaporated to make Ohmic contacts for the measurement structures. Reference devices (without tungsten lines) were fabricated on the same sample by exposing the mesa structure outside the W-patterned areas.

The overgrown patterns were analyzed using transmission electron microscopy (TEM) in order to evaluate the effect of the overgrown patterns on the layer quality. TEM lamellas (about 40 nm thick) were made using focused ion beam/SEM system FEI Nova NanoLab 600 and the inspection was performed with a JEOL 3000F.

a)Electronic mail: gvidas.astromskas@ftf.lth.se

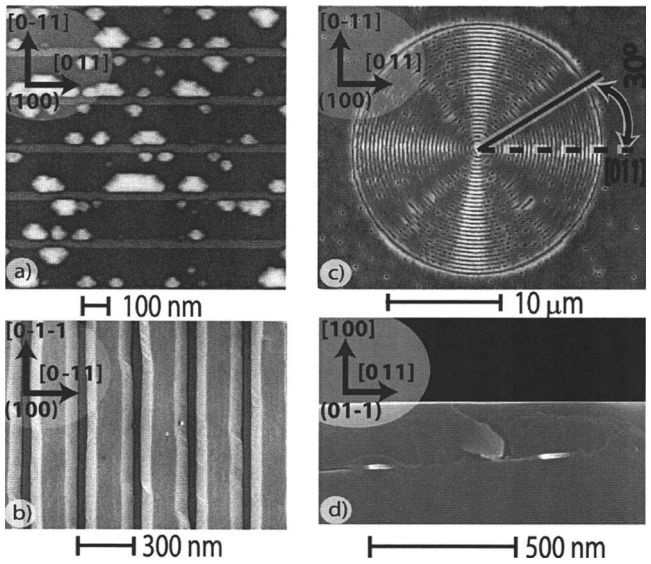

FIG. 1. (a) Formation of Stranski–Krastanow islands along tungsten lines at 600 °C (10 nm deposition). (b) Formation of mesa ridges in between lines at 500 °C (90 nm deposition). (c) Overgrown circle showing preferential overgrowth direction to be 30° of the [011] direction, corresponding to grating directed at 30° from the $[0\bar{1}1]$ direction (290 nm deposition). (d) SEM image of cross section of the overgrown (290 nm deposition) tungsten pattern, with two tungsten lines shown as white contrast.

III. EPITAXIAL GROWTH

Successful homoepitaxial InAs overgrowth over W patterns has been reported when growing at a V/III ratio of 20 and at a growth temperature of 600 °C;[4] therefore we evaluated whether these growth conditions result in overgrowth when InAs is grown on GaAs. But due to the large lattice mismatch, InAs forms Stranski–Krastanow (SK) islands when deposited on a GaAs substrate (Fig. 1). Outside the patterned areas we observed nonuniform island sizes, ranging in diameter from less than 2 nm up to 20 nm for the used growth temperature of 600 °C. In contrast to the unpatterned areas on the same substrate, we found that inside the grating, Fig. 1(a), most islands nucleated along the tungsten lines, with only a very few SK islands forming in between the tungsten lines. Besides, the islands along the tungsten lines were substantially larger in size than the ones in the middle. This indicates that larger islands also had higher growth rate as more material was deposited, preventing surface planarization.[5] In order to reduce size nonuniformity and increase the SK island density, a lower deposition temperature of 500 °C was selected.[6,7] Here, the choice of temperature was crucial, as we found that the use of higher growth temperatures resulted in a rougher surface for the overgrown layer. At the new growth conditions we observed that the deposited InAs (about 70–90 nm thickness) resulted in a flat (001) top surface grown in between lines oriented along the $[0\bar{1}1]$ direction, as shown in Fig. 1(b). This was confirmed by AFM inspection, which also revealed that the side planes extended down to the tungsten grating and had angles of either 45° or 54.6° toward the (001) surface, corresponding to {110} and {111}*A* planes, respectively. Such ridges were

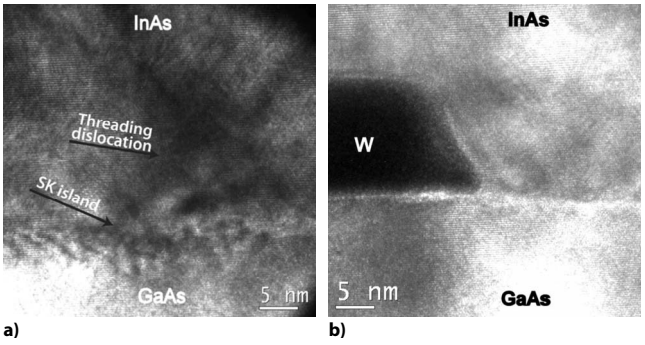

FIG. 2. TEM images of (a) interface between InAs and GaAs of the reference device. (b) Interface between InAs/W/GaAs of the overgrown structure. The arrows mark the SK island and the threading dislocation, originating from the island. The interface of the metal patterned device is smoother and leads to less stacking faults at the interface in between the metal pattern structure.

reported in the homoepitaxial InAs overgrowth at 600 °C.[4] Therefore, the identification of the same shape and direction of the limiting growth planes as in homoepitaxial overgrowth indicates that the strain did not considerably influence the growth of InAs on W-patterned GaAs at the growth temperature used.

The overgrowth of the W and the planarization above the grating were achieved with a thicker InAs layer of 290 nm. The circular patterns of tungsten revealed a strong directional dependence of the InAs growth, as shown in Fig. 1(c). Three clearly distinguishable growth modes in different directions can be identified in the developed patterns above the circles: complete overgrowth, mesa-type ridge formation along the [011] direction, and a mixed region of mesa ridges and partial overgrowth along the $[0\bar{1}1]$ direction. Complete overgrowth of the tungsten occurred when the grating was aligned 30° off the $[0\bar{1}1]$ direction. This direction corresponds to the fast growing facet of InAs.[4] The complete overgrowth was void-free as shown in Fig. 1(d).

IV. TEM RESULTS

High resolution cross-section TEM images in Fig. 2 compare the InAs quality between the reference (a) and the overgrown (b) devices. The location of the interface between InAs and GaAs is easily identified in both images, but the reference in (a) has a wider area of mottled contrast due to Moiré patterns of overlapping lattices with slight misorientation, indicating a much more uneven interface. The contrast in (a) also indicates the formation of a Stranski–Krastanow dot (arrow) with the base at the interface and 60° stacking fault pairs emerging from the top of the dot, which may form the origin of threading dislocations. In the W-patterned sample in (b), the interface was relatively smooth and abrupt and with a much lower density of lattice disturbances in the area in between the dark W patterns. Lattice planes are visible in both images even near the interface, but individual edge dislocations at the interface cannot be identified due to insufficient image quality of the comparably high sample thickness. However, the only threading dislocations, propa-

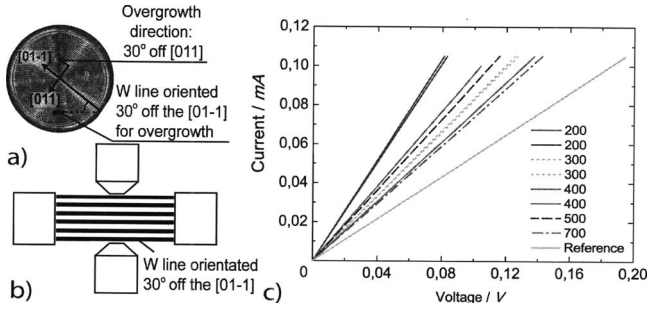

FIG. 3. *IV* characterizations of the overgrown devices. (a) Layout of the directions on the sample. (b) Schematic structure of the overgrown devices. (c) *IV* characteristics of overgrown devices and references. Numbers in the legend stand for the period of the 90-nm-wide tungsten lines.

gating along the {111} direction observed in the patterned device, were in most cases located at the middle of the tungsten mask. The origin of the dislocation at the center of the mask coincides with the coalescence region for the two InAs growth fronts meeting above the W structure.

The InAs lateral overgrowth starts after 15 nm of InAs deposition (height of W) and a better structural quality of the overgrown layer is achieved as compared to the reported heteroepitaxial overgrowth of InAs.[8] Our samples are grown under a low V/III ratio and a low growth temperature to favor the growth on high energy facets that form along the overgrowth direction. We observe that dislocations are more frequent at the unpatterned InAs/GaAs interface, whereas W patterns yield lower defect density in the overgrown layer. However, the overgrown layer is not defect-free, as 60° threading dislocations originating from the coalescing growth fronts create propagating dislocation lines with about one coalescence dislocation per wire. This is in contrast to the TEM results of GaAs overgrowth on W (Ref. 9) and may be attributed to the strain relaxation in the overgrown material.

V. ELECTRICAL CHARACTERIZATION

Electrical measurements were done to evaluate the resistance of the material and to determine the carrier concentration and the carrier mobility. Experiments were carried out on $70\times20\ \mu m^2$ devices (Hall bars) containing embedded gratings oriented 30° off the $[0\bar{1}1]$ direction ("Overgrown devices") and devices without any metal lines ("Reference"). Figure 3(a) illustrates the direction of overgrowth and how tungsten lines should be aligned in order to investigate the electrical properties of the overgrown layer and device schematic is shown in Fig. 3(b).

As shown in Fig. 3(c), the overgrown devices had a lower resistance as compared to the reference and, in total, the resistance was reduced to less than half for the hybrid (InAs/W) devices as compared to the references without any tungsten lines. The mesa geometry was used to deduce the conductivity of the devices from the measured data. Based on reported values for the resistivity for overgrown tungsten lines ($120\ \mu\Omega$ cm),[3] it was calculated that the contribution from the metal accounted only for about 15% (it varied with pattern density from 11% to 18%) of the total measured conductance in our devices. It may hence not be responsible for the observed reduction in the resistance as the metal density increased.

In order to analyze the origin of the low resistance in the overgrown structures, Hall measurements were performed on samples with an InAs thickness of 290 nm at room temperature and at 77 K. Figure 4 shows the deduced values for the carrier densities (a) and mobilities (b) of the fabricated devices. The main results are that the reference structure had a comparably low carrier concentration but a high mobility, while the mobility in the overgrown structures did not exceed 3000 $cm^2/V\,s$. However, all overgrown devices exhibited higher carrier density than the reference structure. The deduced Hall mobility value for the reference InAs layer (4850 $cm^2/V\,s$) corresponds well to the measured mobilities at room temperature for thin InAs layers grown on GaAs.[10] This value increased to 6300 $cm^2/V\,s$ at 77 K, while the mobility for all the hybrid structures remained essentially constant. To remove the influence of the metal, the tungsten conductance was subtracted from the total conductance when calculating the electron mobility. Also, the Hall constant for our sample may be assumed to have contributions from two sources—the tungsten wires and the InAs layer. This can be evaluated using Petritz's approach:[11]

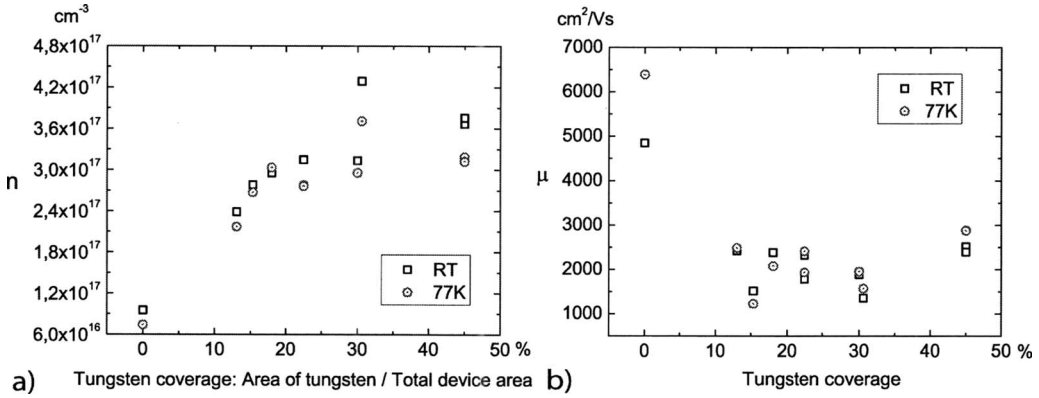

FIG. 4. Hall effect measurement results: (a) carrier density and (b) mobility as a function of the tungsten coverage.

$$R_H = R_{H_W}\frac{d_W}{d}\left(\frac{\sigma_W}{\sigma}\right)^2 + R_{H_{InAs}}\frac{d_{InAs}}{d}\left(\frac{\sigma_{InAs}}{\sigma}\right)^2.$$

Here, R_H is the Hall constant, d is the total layer thickness, and σ is the total conductivity of the hybrid structure. d_W, d_{InAs}, σ_W, and σ_{InAs} are the thicknesses and conductivities of the tungsten wires and the InAs film, respectively. According to the formula, the Hall coefficient for the tungsten was negligible compared to the InAs layer due to the large resistivity of tungsten (ρ=120 $\mu\Omega$ cm).

VI. DISCUSSION

Studies of strained InAs grown on GaAs and Si substrates[10–14] have shown that the deposited layer may be separated into three regions: the interface, the bulk, and the surface. The extent of the interface layer varies with different growth conditions and especially with various attempts to reduce the dislocation density where it can be reduced from 1 μm (Ref. 14) to 200–300 nm.[12] As we have been studying thin InAs layers in our overgrown devices (290 nm), they should consist of only the surface layer and the interface. Lack of any bulk layer, for instance, explains the low value for the mobility of the reference device.

Inserting the tungsten into the InAs layer affects primarily the dislocated interface layer, although a second surface layer may be expected to form around the tungsten lines. As shown in a study with metal-insulator-semiconductor capacitor measurements,[12] the mobility at the surface is heavily dependent upon the total charge in the accumulation region, explaining the reduction in mobility when tungsten is present. Figure 4(a) shows an increased carrier concentration with the addition of tungsten. The possible source for this increase is the accumulation of electrons around the tungsten due to the pinning of the Fermi level in the conduction band. Also, the Hall mobility of the overgrown samples was not decreasing with higher tungsten coverage while the carrier concentration demonstrated a weak increase with the higher W coverage. This relation suggests that the observed reduction in resistance may be attributable to a conducting layer around the W. This conclusion is further supported by other studies of dislocated InAs layers[11–13] that show temperature dependent mobility, which we did not observe in our measurements.

The electrical measurements may be explained considering a simple model where change in the surface from GaAs/InAs-like to W/InAs-like occurs when the tungsten coverage increases. Either interface can be characterized with a specific carrier density or the measured total carrier concentration will be proportional to the area occupied by each surface type. In this case, a linear increase would be expected as observed for a low W coverage [Fig. 4(a)]. The nonlinear dependence of measured carrier concentration can be explained if one assumes that surface regions around neighboring tungsten lines overlap, locally modifying the band bending. In this regime, the electron concentration has a weaker dependence on the coverage. From the TEM inspection we conclude that the dislocation density changes when tungsten is present; therefore one has to take into account a change in dislocation density as well. As most of the tungsten lines inspected in the TEM had a coalescence dislocation related to them, we assume that the number of these dislocations increases linearly for devices with more tungsten lines. One may thus expect that the carrier concentration should increase linearly when more coalescence dislocations are present. However, the carrier concentration, shown in Fig. 4(a), saturates at higher tungsten coverage. Also, the increasing dislocation density should reduce the carrier mobility, but we observed a rather constant trend in the measured Hall mobilities [Fig. 4(b)]. We hence describe a possible electrical transport mechanism for the overgrown hybrid InAs/W/GaAs devices as a combination of surface accumulations, appearing at the InAs surface and at the InAs/W interface, and dislocation scattering. Electrically, this results in the observed increased conductance for the overgrown devices as compared to the reference.

VII. SUMMARY

We studied the conditions for the epitaxial overgrowth of InAs on W–GaAs patterned substrates. It was demonstrated that the InAs preferentially nucleates along the metal patterns and that these nucleation sites form the basis for subsequent lateral overgrowth over the metal. A deposition temperature of 500 °C was preferred as it was sufficiently high to prevent polycrystalline deposition on the metal, while it still provided a high density of nucleation sites and reduced diffusion of In species on the growing surface. A complete, void-free overgrowth with a planarized top surface could be achieved after 290 nm of deposition for a metal grating oriented 30° off the $[0\bar{1}1]$ direction as confirmed with TEM inspection. Hybrid InAs–W–GaAs structures showed a lower resistivity when compared to InAs–GaAs reference devices. An increased carrier concentration in the overgrown structures compensated for the reduced mobility and resulted in a net increase in the conductivity of the overgrown structure.

ACKNOWLEDGMENTS

This work was supported by the Swedish Research Council (VR), the Swedish Foundation for Strategic Research (SSF), and the Knut and Alice Wallenberg Foundation (KAW).

[1] B Y. Ma, J. Bergman, P. Chen, J. B. Hacker, G. Sullivan, G. Nagy, and B. Brar, IEEE Trans. Microwave Theory Tech. **54**, 4448 (2006).
[2] L. Shterengas, G. Belenky, M. Kisin, and D. Donetsky, Appl. Phys. Lett. **90**, 011119 (2007).
[3] L.-E. Wernersson, K. Georgsson, A. Gustafsson, A. Lofgren, L. Montelius, N. Nilsson, H. Pettersson, W. Seifert, L. Samuelson, and J.-O. Malm, J. Vac. Sci. Technol. B **20**, 580 (2002).
[4] L.-E. Wernersson, E. Lind, J. Lembke, B. Martinsson, and W. Seifert, J. Cryst. Growth **280**, 81 (2005).
[5] G. Astromskas and L.-E. Wernersson, J. Phys.: Conf. Ser. **100**, 042043 (2008).
[6] S. Liang, H. L. Zhu, J. T. Zhou, Y. B. Cheng, J. Q. Pan, L. J. Zhao, and W. Wang, Proceedings of the International Symposium on Metamaterials, (2006).
[7] A. A. Khandekar, G. Suryanarayanan, S. E. Babcock, and T. F. Kuech, J. Cryst. Growth **292**, 40 (2006).

[8]G. Suryanarayanan, A. A. Khandekar, T. F. Kuech, and S. E. Babcock, Appl. Phys. Lett. **83**, 1977 (2003).
[9]L.-E. Wernersson, M. Borgstrom, B. Gustafson, A. Gustafsson, L. Jarlskog, J.-O. Malm, A. Litwin, L. Samuelson, and W. Seifert, J. Cryst. Growth **221**, 704 (2000).
[10]P. Sheldon, M. M. Al-Jassim, K. M. Jones, and J. P. Goral, J. Vac. Sci. Technol. A **7**, 770 (1989).
[11]C. Besikci, Y. H. Choi, G. Labeyrie, E. Bigan, M. Razeghi, J. B. Cohen, J. Carsello, and V. P. Dravid, J. Appl. Phys. **76**, 5820 (1994).
[12]T. Iwabuchi, T. Ito, M. Yamamato, K. Sako, Y. Kanayama, K. Nagase, T. Yoshida, F. Ichimori, and I. Shibasaki, J. Cryst. Growth **150**, 1302 (1995).
[13]Z. Hongwei, Z. Yiping, W. Hongmei, D. Jianrong, Z. Zhanping, P. Liang, and K. Meiying, J. Cryst. Growth **191**, 361 (1998).
[14]H. A. Washburn, J. R. Sites, and H. H. Wieder, J. Appl. Phys. **50**, 4872 (1979).